Korean J. Chem. Eng., 37(10), 1726-1731 (2020)
DOI: 10.1007/s11814-020-0580-8

pISSN: 0256-1115
eISSN: 1975-7220

In-situ crystallization of sildenafil during ionic crosslinking of alginate granules

Seungvin Cho*, Jeong Won Kang, and Jonghwi Lee*,†**

*Department of Chemical Engineering and Materials Science, Chung-Ang University,
221 Heukseok-dong, Dongjak-gu, Seoul 06974, Korea
**Department of Chemical and Biological Engineering, Korea University, 145 Anam-ro, Sungbuk-gu, Seoul 02841, Korea
(*Received 28 February 2020 • Revised 9 May 2020 • Accepted 13 May 2020*)

Abstract−Hydrogel particles containing drug crystals were investigated for the development of drug formulations with improved processability, bioavailability, and physical stability. However, crystal engineering inside hydrogel particles has been limited due to various difficulties involved in the preparation processes and their control. This study demonstrates the crosslinking of alginate granules and the simultaneous crystallization of a drug, sildenafil, inside the granules by using a simple and scalable preparation technique. The particle size of the drug crystals was successfully decreased to the submicron range while their crystallinity could be controlled by the processing parameters. Moreover, these results are shown to be due to the strong interactions between the polymer chains and the drug as well as the diffusion-limited processes of solvent, antisolvent, sildenafil, alginate, and crosslinking ions (Ca^{2+}). This simple crystallization technique will be useful for the development of novel drug delivery systems based on hydrogels and drug crystallites.

Keywords: Drug Delivery, Hydrogel, Alginate, Sildenafil, Polymer-directed Crystallization, Granule

INTRODUCTION

For decades, hydrogels have been developed as drug delivery carriers for various purposes such as sustained and fast stimuli-responsive release, enhanced processability, and improved stability [1-3]. The mesh structures of hydrogels can be engineered in a wide range of sizes, which allows for control over both the release behavior and the properties of the drugs loaded inside the hydrogels [2,4]. However, loading a drug into hydrogel particles remains a challenge [5]. When crosslinking conditions are too harsh for a drug, the crosslinking of particles in the presence of a preloaded drug is not preferred [6]. The post-loading of drugs into a crosslinked hydrogel particles is not straightforward either, particularly if the drugs are hydrophobic and require the use of an organic solvent [7], since hydrogels are intrinsically hydrophilic. Furthermore, loading a drug in its controlled crystalline state, which has better physical stability compared to its amorphous or liquid states, into hydrogels is even more difficult [8].

To date, only a few studies have been reported on the development of a method to load hydrogel particles with drug crystals. Fenofibrate was crystallized inside core-shell particles of alginate hydrogel, via controlled evaporation, resulting in sub-nanometer sized crystals [9]. This process was possible only after creating a stable nano-emulsion of fenofibrate, alginate, and polyvinyl alcohol by ultrasonication, which is a delicate process. However, the crystallization behavior and the particle sizes of the obtained crystals were not analyzed. Alginate was also used as a binder in the spherical crystallization of drugs by dropping drug/alginate solutions into an antisolvent [10]. Unfortunately, the crystal size was not analyzed either and only the conventional X-ray powder diffraction (XRD) results, similar to those obtained from the regular antisolvent crystallization, were reported. Moreover, no interactions between the alginate and the drugs were reported in this study. Alginate microparticles were also utilized as additives (heteronucleants) to control the nucleation of drug crystals formed during cooling crystallization [11,12]. In this case, loading of the drug into the microparticles was only controlled through bulk nucleation and equilibrium partitioning, which are intrinsically difficult to control. Still, these previous studies did elucidate some details on the confinement effect and diffusion-limited crystallization. However, the structures of engineered particle and crystals were not investigated properly and, to the best of our knowledge, no attempt to uncrosslink the networks for the analysis of the loaded crystals has been made.

In this study, a convenient and scalable process that can produce hydrogel granules containing drug crystals was developed. These hydrogel granules are large enough for post-unit operations such as blending, milling, compaction, and tableting [13], while the drug crystals are small enough to show improved dissolution characteristics [14-16]. In this study, droplets of an aqueous alginate solution were simply injected into a drug solution of an organic solvent containing an alginate crosslinking agent. The inter-diffusion of the two phases simultaneously triggered the crystallization of the drug and the crosslinking of alginate hydrogel particles. The resulting crystals were successfully analyzed after uncrosslinking. Sildenafil citrate, a PDE type 5 inhibitor, was chosen as a model drug for this crystallization study, and it resulted in a significant particle size reduction (Fig. 1) [17].

Particle size reduction methods have been introduced in attempts to overcome the problems related to the poor water solubility of drugs [18-21]. Although many techniques have been developed,

†To whom correspondence should be addressed.
E-mail: jong@cau.ac.kr

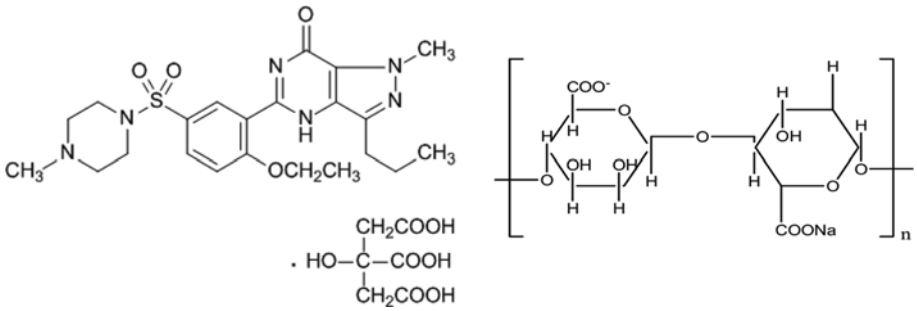

Fig. 1. Chemical structures of sildenafil citrate (left) and sodium alginate (right).

most of them require delicate post-processes due to the poor processability of small crystals [14,22,23]. For example, removing the water medium used for nanocrystal preparation often induced severe aggregation [24,25] and as a result, carefully developed drying techniques are often employed [26-28]. Hence, if small crystals could be prepared inside hydrogel particles of relatively large sizes, i.e., granules, improved processability for the subsequent unit operations could be achieved. Herein, the interactions between the macromolecular chains of the hydrogels and the drug enables particle size engineering, which is similar to 'polymer-directed crystallization' [29-33].

EXPERIMENTAL

1. Materials

Sildenafil citrate was purchased from Cadila Pharmaceuticals (GMP, Ahmedabad, India). Sodium alginate (Sigma Aldrich, St. Louis, MO, USA), calcium chloride dehydrate (extra pure, Duksan Pure Chem., Incheon, Republic of Korea), NH_4Cl (99.5%, Daejung Chem., Gyeonggi, Republic of Korea), and dimethyl sulfoxide (DMSO, 99.8%, SamChun Pure Chem., Gyeonggi, Republic of Korea) were used. All chemicals were used as received without further purification.

Table 1. Properties of sildenafil crystallized by antisolvent (water) addition into DMSO (*yield=amount in hydrogel/total amount of drug used)

Designation	Preparation conditions		Particle size (μm)	Yield in hydrogel (wt%)*	T_m (°C)	ΔH (J/g)
	Drug : alginate (wt ratio)	$CaCl_2$ (wt%)				
S	10 : 0	0	11.4 (±2.8)	-	190.4	270
SA	10 : 1	0	8.7 (±1.9)	-	187.4	50
SAC1	10 : 1	0.45	1.7 (±0.1)	32.8 (±0.9)	182.7	310
SAC5	10 : 1	2.22	0.9 (±0.2)	51.5 (±0.5)	-	-
SAC1(rev)	10 : 1	0.45	4.4 (±0.8)	53.7 (±0.5)	186.2	160

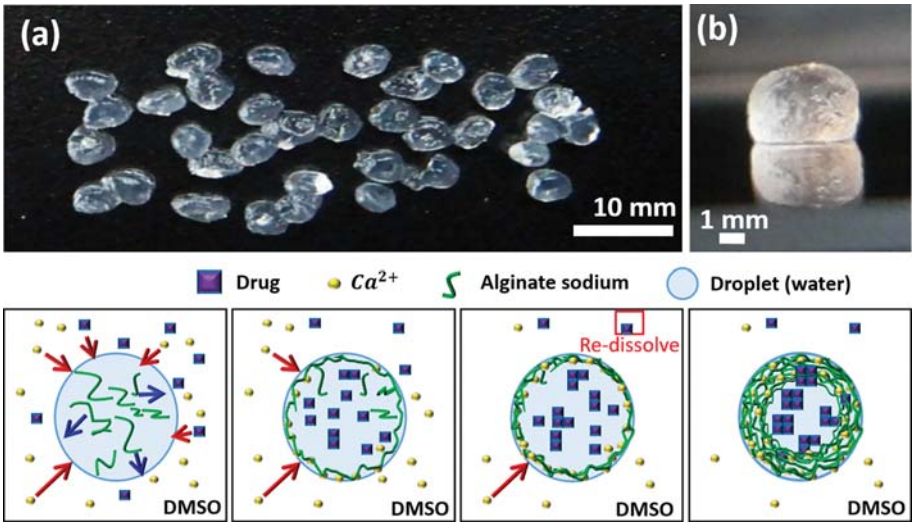

Fig. 2. (a) Top image of SAC1 and (b) side image of SAC1 granules on a glass plate (upper). Formation mechanism of hydrogel granules (lower); the red and blue arrows indicate the flux of DMSO and water with their dissolved molecules, respectively.

2. Drowning-out Crystallization and Granule Formation

Sildenafil citrate (0.1 g/mL) and $CaCl_2$ were dissolved in DMSO (Table 1) in a 5 mL beaker with magnetic stirring at 300 rpm. The sildenafil was crystallized at 25 °C by the injection of 1 mL of a 1 wt% aqueous sodium alginate solution into 1 mL of the DMSO solution (feed rate of 1 mL/h). A single syringe injection pump (KDS-100, Kd scientific, Massachusetts, USA) and a nozzle with a 0.8 mm internal diameter were used. For reverse drowning-out crystallization, the DMSO solution of sildenafil citrate and $CaCl_2$ was injected into the aqueous alginate solution at the same feed rate (SAC1(rev) in Table 1). Granular particles were recovered by filtration after crystallization (PTFE (hydrophilic), 0.45 mm, Hyundai Micro, Republic of Korea) (Fig. 2).

3. Characterization

The drug crystals in the granules were separated by uncrosslinking the alginate hydrogels in a 1 M aqueous solution of NH_4Cl (30 mL for a crystallization batch) at 25 °C under magnetic stirring at 700 rpm for 3 h. The solution was subsequently filtered using the same PTFE membranes as above. Dried crystals were observed by scanning electron microscopy (SEM, S-3400, Hitachi, Japan) after carbon coating (carbon coater, Hitachi, Japan; 120 sec). Volume-average particle size and particle size distribution were analyzed by a laser light scattering particle size analyzer, under stirring of 340 mL/min, after sonication (40 W, 39 Hz) for 3 min (LA-910, Horiba, Kyoto, Japan; medium 150 mL of 1 M NH_4Cl aq. solution, 1.61 relative refractive index). The crystallinity of the drug crystals was examined by X-ray diffraction (XRD, SmartLab, Rigaku, Japan) at a scan rate of 1.2°/min. The solution-mediated transformation of amorphous phases was monitored after storage at 70 °C and 75 RH%. Their thermal properties were assessed by differential scanning calorimetry by heating 4.6-5 mg of a powder sample from 30 to 180 °C at a rate of 5 °C/min (DSC, DSC-Q1000, TA Instrument, UK). Interactions between molecules were investigated by attenuated-total-reflectance Fourier-transform infrared spectroscopy with a scan number of 1000 (ATR-FTIR, Nicolet 6700, Thermo Scientific, Waltham, MA, USA).

RESULTS AND DISCUSSION

1. Formation of Granular Hydrogels

The typical mesh structures of Ca-crosslinked alginates (average pore diameters of ca. 14-17 nm) are known to significantly interfere with the diffusion of molecules with molar masses between 44-155 kD, which is a function of various conditions such as the concentration of Ca ions, type of alginate, etc [34,35]. But, these interferences are relatively small for molecules with low molecular weights, such as sildenafil, Ca^{2+}, solvent, and antisolvent. Therefore, upon contact between the two solutions, the alginate is crosslinked by the relatively fast diffusion of the Ca ions. Moreover, even after the surfaces of alginate droplets are crosslinked, the alginate chains do not significantly interfere with the inter-diffusion process of sildenafil, Ca^{2+}, solvent, and antisolvent, resulting in further crosslinking and crystallization. Figs. 2(a) and 2(b) show images of the alginate granules, and it can be seen that they are in the mm size range. Moreover, the alginate chains have the slowest diffusion rate among the molecules and thus, as a natural consequence, the size of alginate granules is determined by the size of droplets generated by the nozzle of the antisolvent. Furthermore, when placed on the surface of a glass plate, the spherical structure of the granules is lost as the bottom surface of the granules is flattened due to gravity, indicating a low crosslinking density and a high swelling ratio. In addition, the cloudy color indicates the existence of multiple phases inside the granules.

2. Crystallization of Sildenafil

The crystallization behavior of a sildenafil control sample was first examined by following the same crystallization procedure but without using alginate and $CaCl_2$ (S in Table 1). The conventional antisolvent crystallization of sildenafil, using DMSO and water, produced crystals of acicular morphology with a particle size of 11.4 μm (Fig. 3(a)). In the presence of alginate, however, the crystal morphology drastically changed to a plate morphology while the average particle size slightly decreased to 8.7 μm (Fig. 3(b) and Table 1). These results of polymer-directed crystallization indicate that there exist significant intermolecular interactions between the alginate and sildenafil that lead to the possible surface adsorption of alginate chains and the alteration of the crystal growth path [33,36,37].

With the addition of $CaCl_2$ into the DMSO phase (SAC1 and SAC5), alginate granules are formed and the crystallization inside these granules results in smaller angular-shaped particles of low aspect ratios (Figs. 3(c) and 3(d), and Table 1). Moreover, increasing the $CaCl_2$ concentration yielded more tightly crosslinked alginate hydrogel granules, which resulted in much smaller submicron

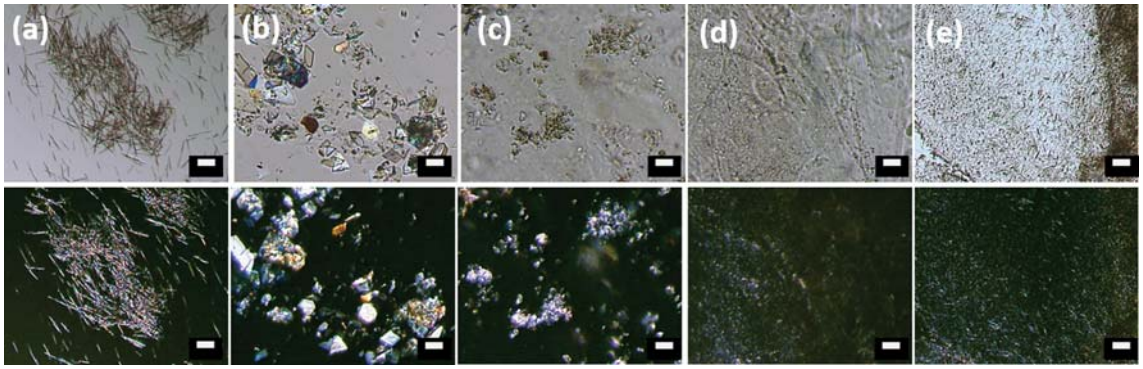

Fig. 3. Optical microscope images of sildenafil crystals without (upper) and between (lower) crossed polarizers: (a) S, (b) SA, (c) SAC1, (d) SAC5, and (e) SAC1(rev) (scale bar=30 μm).

particle sizes (SAC5). In this case, no individual particles could be identified under an optical microscope, but optical birefringence originating from the crystallinity was still confirmed. Particles recovered by uncrosslinking the alginate networks were characterized by SEM, and small angular-shaped particles, similar to cubic particles, were observed (Fig. 4). The decrease in particle size with increasing Ca ion concentration was confirmed as well. In addition, the existence of crystallinity could also be conjectured from the appearance of angular particles (crystal habit). The results of the size analysis by light scattering, which are generally consistent with the results of SEM, showed bimodal distributions that are possibly due to the aggregation of crystals (Fig. S1). A significant percentage of particles exhibit submicron sizes. The retarded crystal growth of sildenafil by alginate chains in this study is similar to previous results of the retarded crystallization of lactose in the presence of alginate [38].

While the granules are forming, the crystal nucleation of sildenafil is likely initiated at the interfaces, resulting in crystals being found in both the granule (hydrogel) and the liquid phases. Initially, the sildenafil molecules exist in the liquid DMSO phase outside the water droplets, and as they diffuse into the water droplets, crystal nuclei form near the interface between the water and the DMSO which then grow into crystals (Fig. 2 schematic diagram). Furthermore, the water molecules diffusing out of the droplets could also trigger crystal nucleation near the interfaces, but the resulting crystals easily re-dissolve into the DMSO phase as the water mixes with the excess DMSO. However, with a further increase in the water concentration, the nucleation and growth of sildenafil crystals are initiated in the DMSO liquid phase. This study focuses on the crystals formed inside the granules as they can easily be recovered by filtration.

In the analysis of SAC1, the amount of sildenafil crystals inside the alginate granules was 32.8 wt% of total the sildenafil used. This was measured by the weight of crystals separated from the hydrogel phases (Table 1, yield, three replicates). The number of crystals obtained from the DMSO liquid phase after filtering was 66.4± 1.4 wt%. Therefore, 99.2 wt% of the sildenafil was recovered as crystals, while possible damage to the crystals during uncrosslinking by surface dissolution appears to be negligible (Fig. S2). Moreover, the yield in the hydrogel improved by increasing the Ca ion concentration (51.5 wt% in SAC5) (Table 1).

The crystallization conditions, such as different nozzle sizes, feed rates of antisolvent, mixing speeds, and concentrations of the alginate solution, were quickly verified by optical microscopy of the crystals (Figs. S3-S6). It was found that these processing parameters did not create such distinct differences as those shown in Fig. 3 and, as a result, most experiments were performed at these fixed conditions. While different nozzle sizes, mixing speeds, and concentrations of alginate solution did not create significant differences in Figs. S3-S5, a marginal increase in particle size was noticed as the feed rate of the solvent decreased (Fig. S6). The slower feed rate likely results in a longer growth time for the crystals in the granules. Furthermore, when pectin was used instead of alginate, the formation of granules and the crystallization of sildenafil inside the granules appeared to be similar (Fig. S5(c)).

3. Reverse Drowning-out Crystallization

In the case of the reverse drowning-out crystallization [SAC1(rev)], similar granules containing sildenafil crystals formed. Upon contact of the DMSO droplets with the aqueous alginate solution, crosslinking of the alginate occurred at the interfaces while the drug molecules loaded inside the granules crystallized with the diffusion of water into the granules. The diffusion of sildenafil molecules out of the droplets also triggered crystal growth, which resulted in the formation of large acicular crystals similar to those observed in Fig. 3(a) (Fig. S7). Compared to the case of SAC1, a relatively higher yield was achieved in the hydrogel as the sildenafil molecules were already present inside the droplets from the beginning. Moreover, the average particle size and crystallinity was greater than that of SAC1, which indicates more crystal growth (Table 1).

4. Crystal Structures

The crystal structure of recrystallized sildenafil (S) was confirmed by XRD and found to be form I of sildenafil citrate and not that of sildenafil free base (Fig. 5) [39]. With the addition of alginate, however, the result shows the typical structure of sildenafil free base [39]. In this case, the citrate counter ions seem to detach during crystallization in the presence of sodium alginate. The presence of alginate hydrogels crosslinked by Ca^{2+} ions significantly broadened the XRD peaks of sildenafil. Although the peaks are broad, SAC1(rev) shows the peaks associated with sildenafil crystals. Furthermore, the limited crystallization inside the SAC1 granules appears to produce significantly smaller crystallites and a significant amount of amorphous phase. With an increase in $CaCl_2$ concentration (much higher crosslink density), a further decrease in crystal size and a further increase in amorphous phase content

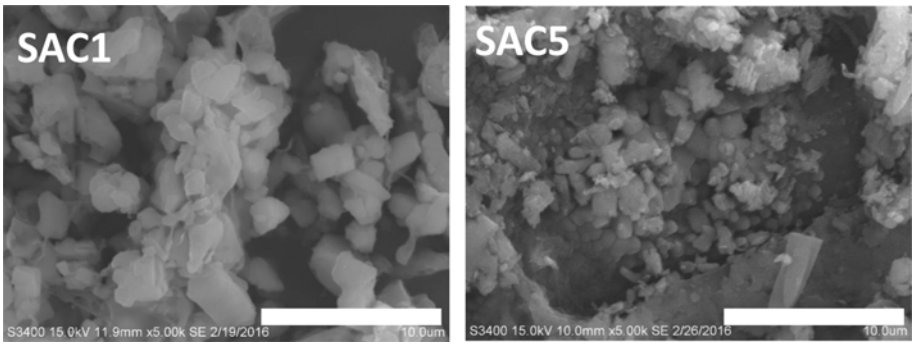

Fig. 4. SEM images of sildenafil particles obtained after removing Ca-alginate hydrogel in SAC1 and SAC5 (scale bar=10 μm).

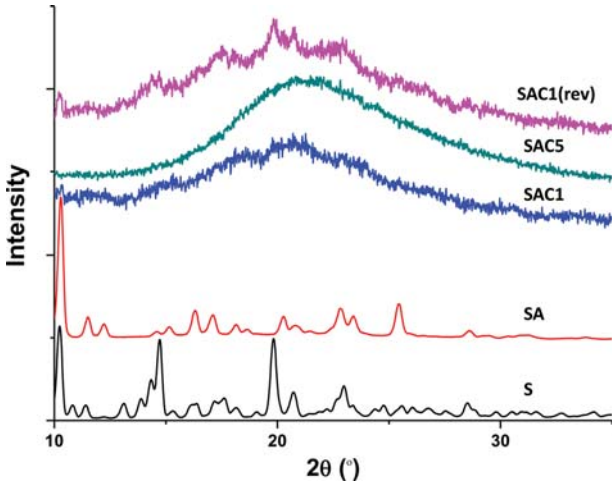

Fig. 5. XRD patterns of powders obtained from different crystallization conditions.

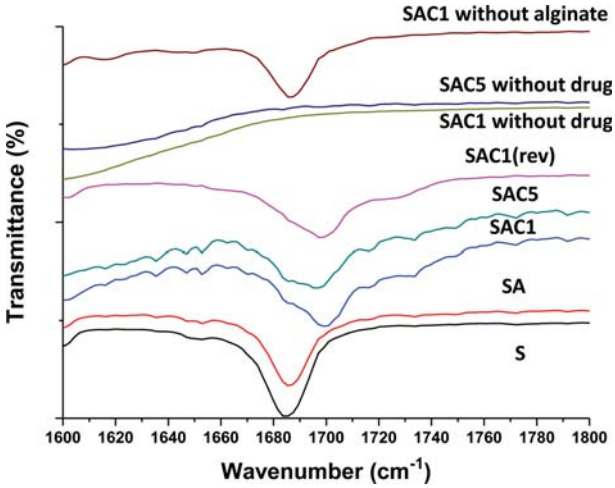

Fig. 7. FT-IR spectra of powders obtained from different crystallization conditions, which show asymmetric C=O stretching peaks.

is observed.

In addition, if the dispersion was stored for more than 12 h after the complete injection of the antisolvent, the amorphous phase inside the granules transformed into crystals (Fig. S8). Since there were only slight changes in the XRD peaks after 12 h, this solution-mediated transformation from amorphous to crystalline phases was almost complete in 12 h. Thus, in addition to crystallization parameters such as $CaCl_2$ concentration, this solution-mediated transformation could be another way of controlling the crystallinity of sildenafil.

5. Thermal Characteristics

Although the XRD patterns of SAC1, SAC5, and SAC1(rev) were largely indicative of an amorphous-like structure, the characteristic optical birefringence of a crystalline phase could be identified in optical microscopy (Fig. 3). Consequently, thermal characterization revealed the existence of melting peaks in the cases of SAC1 and SAC1(rev), whereas SAC5 did not show such a melting transition (Fig. 6). Thus, as conjectured from their XRD patterns, SAC1 and SAC5 exhibit different degrees of crystallinity. Also, the melting points of the crystals inside the granules were significantly lower, by 4.2-7.7 °C, compared to that of recrystallized sildenafil (Table 1). Furthermore, the crystallinities of SAC1 and SAC1(rev), as assessed from the melting enthalpy results, are not that much smaller compared to the recrystallized sildenafil (Table 1). Therefore, although the XRD patterns are broad, the amorphous contents are not dominant. These results also indicate that particle size reduction has a significant influence on the broadening of XRD peaks. Moreover, the influence of particle size reduction could possibly be stronger than the influence of amorphous phase formation. Also, the size of the single-crystal domains could be even smaller than Fig. 4 shows.

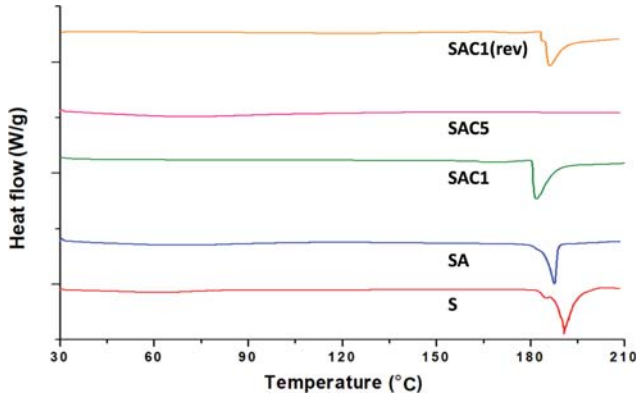

Fig. 6. DSC results of powders obtained from different crystallization conditions.

6. Molecular Interactions

The FT-IR peaks of asymmetric C=O stretching further confirm the molecular interaction between sildenafil and the alginate. Fig. 7 shows a slight shift in the peak position of SA compared to that of S. In the cases of SAC1, SAC5, and SAC1(rev), the ionically crosslinked networks of alginate show distinct shifts towards higher energies (higher wavenumbers) with the addition of $CaCl_2$, which indicates tighter hydrogen bonding between the alginate chains and sildenafil. The prepared controls, alginate hydrogels themselves without sildenafil (data not shown), SAC1 without sildenafil, and SAC5 without sildenafil, which were prepared following the same procedures without using sildenafil, showed no significant peak in the wavenumber range (Fig. 7). Therefore, only sildenafil has a peak in the region. Crystals obtained without using alginate but with $CaCl_2$, i.e., SAC1 without alginate, did not produce any peak shift either. Therefore, the interaction between sildenafil and alginate is the main reason for the peak shifts seen in Fig. 7. This interaction could be responsible for the unique crystallization behavior of sildenafil inside the granules.

It has been shown that the network structure of a hydrogel can slow the diffusion of the crystallizing molecules and affect the crystallization behavior of a drug [9,40]. The crystallization behavior of sildenafil investigated in this study was also significantly influenced by the molecular interactions between sildenafil and the alginate network. As a result, the sizes of the crystal phases could be signifi-

cantly reduced to the sub-nanometer range with depressed melting points. Therefore, both the crystallinity and the particle size of a drug could be engineered in a wide variety inside the granules, while the granules themselves could easily be processed into various drug dosage forms. This crystallization process could readily be adopted by conventional industrial crystallization facilities without expending any extra energy for producing nano-dispersion or nano-emulsions.

CONCLUSIONS

Herein, a novel and simple preparation technique for hydrogel granules containing drug crystallites was developed. The crystallization of sildenafil was triggered upon mixing of water and DMSO droplets containing alginate chains and a drug solution, while the inter-diffusion of solvents, alginate, drug, and Ca ion resulted in *in-situ* crystallization during crosslinking. It was shown that the particle size of sildenafil was significantly reduced to the submicron range, while the size of the granules was large enough for good processability. It was also shown that the crystallinity of the drug could be controlled in a wide range by controlling the processing parameters. This scalable and versatile technique could be conveniently utilized for the development of commercial hydrogel delivery systems for future applications.

ACKNOWLEDGEMENTS

This work was supported by the South Korean National Research Foundation and Ministry of Science, ICT and Future Planning (ERC 2014R1A5A1009799).

SUPPORTING INFORMATION

Additional information as noted in the text. This information is available via the Internet at http://www.springer.com/chemistry/journal/11814.

REFERENCES

1. C. Ma, Y. Shi, D. A. Pena, L. Peng and G. Yu, *Angew. Chem. Int. Ed.*, **54**, 7376 (2015).
2. P. I. Lee, *J. Controlled Release*, **2**, 277 (1985).
3. B. S. Kim, J. Leong, S. J. Yu, Y. Cho, C. G. Park, D. H. Kim, E. Ko, S. G. Im, J. Lee and Y. J. Kim, *Small*, **15**(21), 1900765 (2019)
4. J. Zhou, G. Wang, L. Zou, L. Tang, M. Marquez and Z. Hu, *Biomacromolecules*, **9**, 142 (2007).
5. M. J. Serpe, K. A. Yarmey, C. M. Nolan and L. A. Lyon, *Biomacromolecules*, **6**, 408 (2005).
6. D. Juric, N. A. Rohner and H. A. von Recum, *Macromol. Biosci.*, **19**, 1800246 (2019).
7. H. Lee, Y. Jeong and T. G. Park, *Biomacromolecules*, **8**, 3705 (2007).
8. L. Wu, J. Zhang and W. Watanabe, *Adv. Drug Deliv. Rev.*, **63**, 456 (2011).
9. A. Z. M. Badruddoza, P. D. Godfrin, A. S. Myerson, B. L. Trout and P. S. Doyle, *Adv. Healthc. Mater.*, **5**, 1960 (2016).
10. T. Gu, E. W. Yeap, Z. Cao, D. Z. Ng, Y. Ren, R. Chen, S. A. Khan and T. A. Hatton, *Adv. Healthc. Mater.*, **7**, 1700797 (2018).
11. D. A. Acevedo, J. Ling, K. Chadwick and Z. K. Nagy, *Cryst. Growth Des.*, **16**, 4263 (2016).
12. H. B. Eral, V. López-Mejías, M. O'Mahony, B. L. Trout, A. S. Myerson and P. S. Doyle, *Cryst. Growth Des.*, **14**, 2073 (2014).
13. J. E. Mealy, J. J. Chung, H. H. Jeong, D. Issadore, D. Lee, P. Atluri and J. A. Burdick, *Adv. Mater.*, **30**, 1705912 (2018).
14. J.-Y. Choi, J. Y. Yoo, H.-S. Kwak, B. U. Nam and J. Lee, *Curr. Appl. Phys.*, **5**, 472 (2005).
15. L. Gao, G. Liu, J. Ma, X. Wang, L. Zhou, X. Li and F. Wang, *Pharm. Res.*, **30**, 307 (2013).
16. C. M. Keck and R. H. Müller, *Eur. J. Pharm. Biopharm.*, **62**, 3 (2006).
17. L.-L. Shia, W.-J. Xua, Q.-R. Caoa, M. Yanga and J.-H. Cui, *J. Pharm. Sci.*, **69**, 327 (2014).
18. B. Van Eerdenbrugh, G. Van den Mooter and P. Augustijns, *Int. J. Pharm.*, **364**, 64 (2008).
19. Y. Lu, Y. Lv and T. Li, *Adv. Drug. Deliver. Rev.*, **143**, 1 (2019).
20. Z. Chai, D. Ran, L. Lu, C. Zhan, H. Ruan, X. Hu, C. Xie, K. Jiang, J. Li and J. Zhou, *ACS Nano*, **13**, 5591 (2019).
21. V. K. Pawar, Y. Singh, J. G. Meher, S. Gupta and M. K. Chourasia, *J. Controlled Release*, **183**, 51 (2014).
22. J. Lee and Y. Cheng, *J. Controlled Release*, **111**, 185 (2006).
23. V. Braig, C. Konnerth, W. Peukert and G. Lee, *Int. J. Pharm.*, **554**, 54 (2019).
24. N.-O. Chung, M. K. Lee and J. Lee, *Int. J. Pharm.*, **437**, 42 (2012).
25. D. G. Lim, J. H. Jung, H. W. Ko, E. Kang and S. H. Jeong, *ACS Appl. Mater. Interfaces*, **8**, 23558 (2016).
26. M. K. Lee, M. Y. Kim, S. Kim and J. Lee, *J. Pharm. Sci.*, **98**, 4808 (2009).
27. S. Kim and J. Lee, *Int. J. Pharm.*, **397**, 218 (2010).
28. W. W. L. Chin, J. Parmentier, M. Widzinski, E. H. Tan and R. Gokhale, *J. Pharm. Sci.*, **103**, 2980 (2014).
29. S. K. Poornachary, G. Han, J. W. Kwek, P. S. Chow and R. B. Tan, *Cryst. Growth Des.*, **16**, 749 (2016).
30. V. López-Mejías, J. L. Knight, C. L. Brooks III and A. J. Matzger, *Langmuir*, **27**, 7575 (2011).
31. D. S. Frank and A. J. Matzger, *Cryst. Growth Des.*, **17**, 4056 (2017).
32. M. K. Lee, H. Lee, I. W. Kim and J. Lee, *Die Pharmazie*, **66**, 766 (2011).
33. H. Choi, H. Lee, M. K. Lee and J. Lee, *J. Pharm. Sci.*, **101**, 2941 (2012).
34. R. H. Li, D. H. Altreuter and F. T. Gentile, *Biotechnol. Bioeng.*, **50**, 365 (1996).
35. E. Favre, M. Leonard, A. Laurent and E. Dellacherie, *Colloids Surf., A: Physicochem. Eng. Aspects*, **194**, 197 (2001).
36. R. Q. Song and H. Cölfen, *Adv. Mater.*, **22**, 1301 (2010).
37. H. Lee and J. Lee, *J. Ind. Eng. Chem.*, **21**, 1183 (2015).
38. H. Takeuchi, T. Yasuji, H. Yamamoto and Y. Kawashima, *Pharm. Dev. Technol.*, **5**, 355 (2000).
39. P. Melnikov, P. P. Corbi, A. Cuin, M. Cavicchioli and W. R. Guimarães, *J. Pharm. Sci.*, **92**, 2140 (2003).
40. M. Xia, S.-M. Kang, G.-W. Lee, Y. S. Huh and B. J. Park, *J. Ind. Eng. Chem.*, **73**, 306 (2019).

Supporting Information

In-situ crystallization of sildenafil during ionic crosslinking of alginate granules

Seungvin Cho*, Jeong Won Kang, and Jonghwi Lee*,†**

*Department of Chemical Engineering and Materials Science, Chung-Ang University,
221 Heukseok-dong, Dongjak-gu, Seoul 06974, Korea
**Department of Chemical and Biological Engineering, Korea University, 145 Anam-ro, Sungbuk-gu, Seoul 02841, Korea
(*Received 28 February 2020 • Revised 9 May 2020 • Accepted 13 May 2020*)

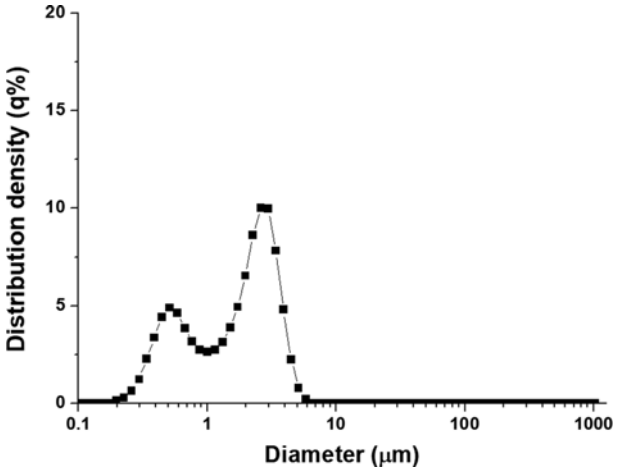

Fig. S1. Particle size distribution of SAC1 obtained from the laser light scattering analyzer (volume average particle size=1.7 μm).

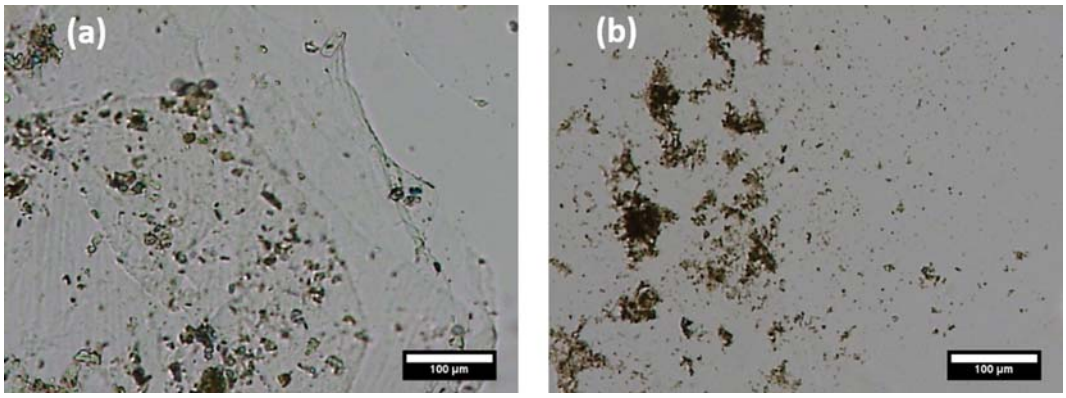

Fig. S2. Optical microscope images without (left) and between (right) crossed polarizers of crystals formed inside hydrogel phases before (a) and after (b) uncrosslinking of alginate.

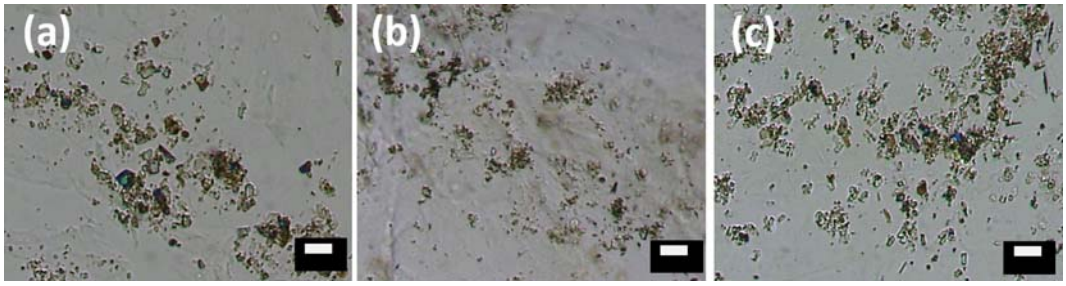

Fig. S3. Optical microscope images of SAC1 prepared by using antisolvent nozzles of different sizes; (a) 0.4 mm, (b) 0.8 mm, and (c) 4.5 mm (scale bar=30 μm).

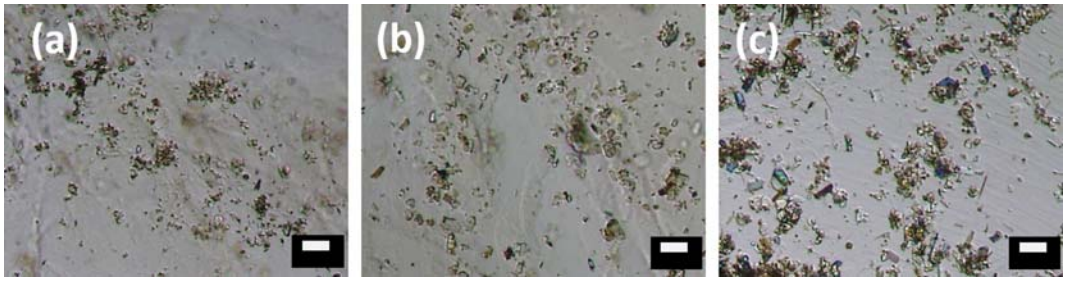

Fig. S4. Optical microscope images of SAC1 prepared by using different agitation speeds: (a) 300 rpm, (b) 500 rpm, and (c) 1,000 rpm (scale bar=30 μm).

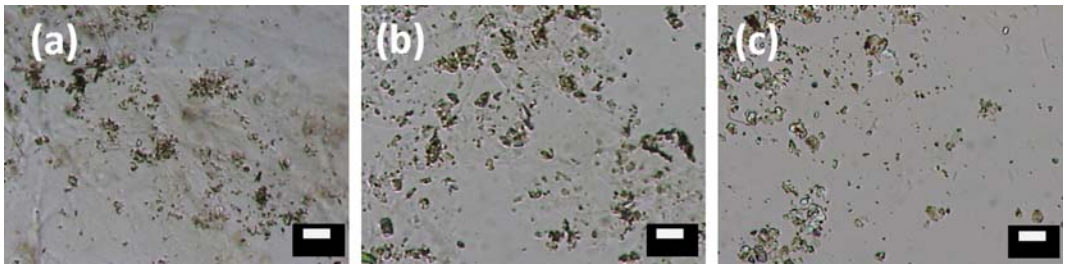

Fig. S5. Optical microscope images of hydrogel granules prepared by different anti-solvents: (a) 1 wt% alginate aq. solution (SAC1); (b) 2 wt% alginate aq. solution; (c) 1 wt% pectin aq. solution (scale bar=30 μm).

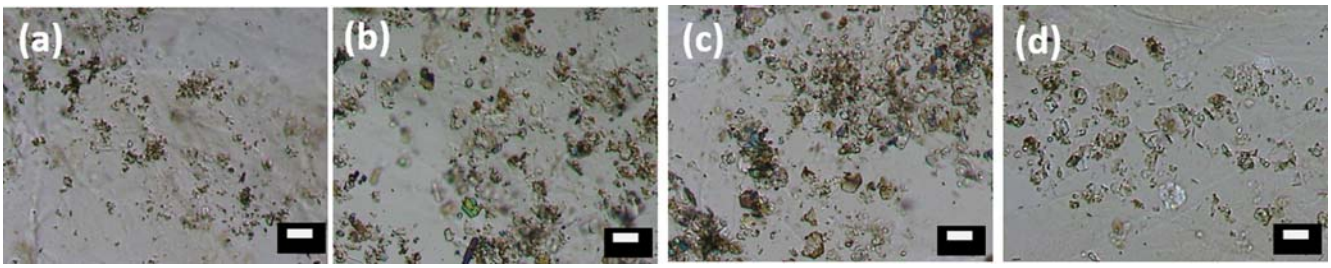

Fig. S6. Optical microscope images of SAC1 prepared by using different feed rates of antisolvent: (a) 1 ml/hr, (b) 0.5 ml/hr, (c) 0.2 ml/hr, and (d) 0.1 ml/hr (scale bar=30 μm).

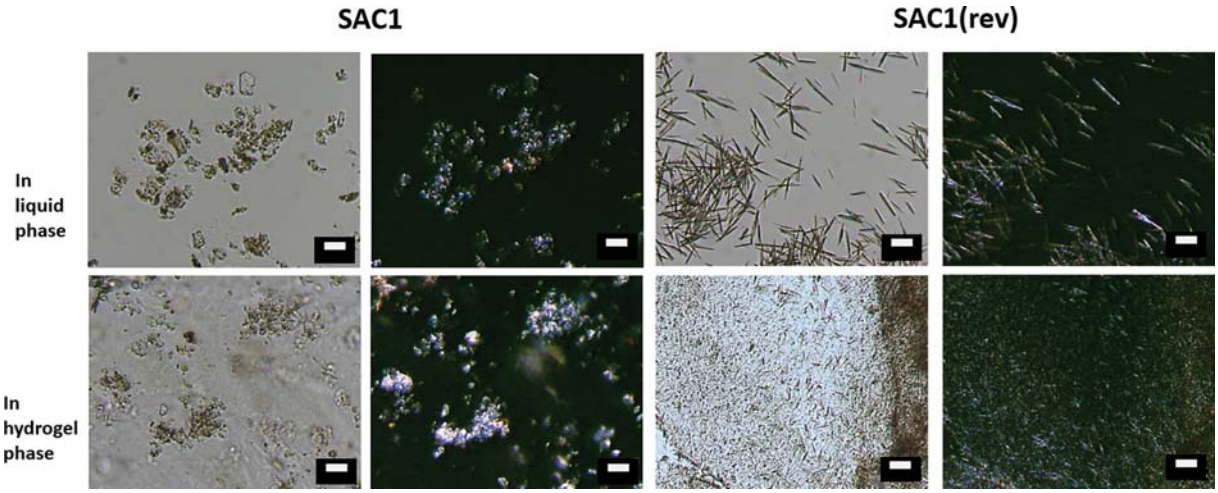

Fig. S7. Optical microscope images of crystals in liquid phases (upper) and hydrogel granules (lower) by different crystallization conditions (scale bar=30 μm).

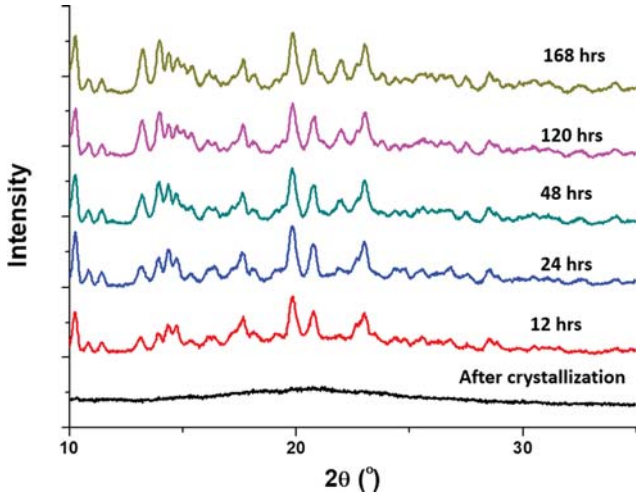

Fig. S8. XRD patterns of SAC1 sample with time stored at 70 °C and 65 RH%.